Journal of Materials Science & Surface Engineering, 5(6): 647-652
ISSN (Online): 2348-8956; 10.jmsse/2348-8956/5-6.2

Finite Element Simulation of the Machining Process with Different Tool Geometries, using Lagrangian Mesh and Johnson-Cook Material Model

Ambrish Singh[1] . B.R. Rawal[2] . M. Chouksey[2] . Vinod Pare[2]

[1]Department of Industrial Production Engineering, SGSITS Indore (M.P.), India.
[2]Department of Mechanical Engineering, SGSITS Indore (M.P.), India.

ABSTRACT
Machining is one of the most common manufacturing processes. It relies on the principle of material removal through forced relative motion between the workpiece and the tool. The primary cause of material deformation in machining is 'Shear' however, in most cases some amount of compressive deformation is also involved. Simulation of this process using Finite Element Method is a challenging task as the process involves material Non-Linearity and significant geometric changes. The use of Lagrangian Mesh with Element deletion governed by, Johnson-Cook material model was adopted for the analysis presented here. Using the explicit solver of ABAQUS (ver. 6.13-1) software the analysis was performed for three different values of Tool Rake Angle, four different value of Tool Nose Radius and two different values of ' depth of cut'. The results obtained from the analysis showed that, with the decrease in the tool rake angle and with an increase in the nose radius the cutting force increases. Also, the observations of chip morphology as presented by the analysis were in agreement with the experimental observations and outcomes, thereby, validating the model.

NCMDMM-2017, August 3-5, 2017, Karnataka, India.

ARTICLE HISTORY
Received 10-07-2017
Revised 19-07-2017
Accepted 29-07-2017
Published 28-08-2017

KEYWORDS
Finite Element Method,
Johnson-Cook,
ABAQUS,
Machining

Introduction

The process machining is perhaps one of the most common manufacturing processes. It has been established that for most of the relevant products in the market, the cost machining has a major part in the final cost of the product. A machining process, in general, works on the idea of material removal through relative motion between the workpiece and the tool. The process is highly non-linear in nature as the workpiece is subjected to high material deformations along with changes in material properties during machining. Apart from nonlinear nature there are several physical aspects of machining like heat transfer, material hardening, residual stress development etc. Each aspect can have a significant impact over the other and can affect the entire process of machining. The development in the field of computer algorithms is not sufficient enough to link these aspects into one holistic model [1]. Therefore, in order to simplify the process of modeling only the cutting force and chip morphology is investigated here.

There are many machining processes but, the discussion presented here is restricted to only those processes that are carried out using a HSS single point cutting tool. The ideas however, can be extended in a limited sense to multipoint cutting tools by incurring certain assumptions. The simulation presented here is that for 3 dimensional shaping operation where, the workpiece is rigidly held in a vice and tool is made to traverse the length of the workpiece with a certain amount of 'depth of cut' as specified by the operator.

Cutting Force Models

The cutting forces in machining play a vital role in overall quality and efficiency of the operation. The study of cutting forces using finite element method can be carried out using methods such as Lagrangian Formulation [2], Arbitrary Lagrangian and Eulerian Formulation [3], Smooth Particle Formulation [4] etc.

In the Lagrangian mesh description, the motion of the mesh is associated with material points. As the material moves, the mesh moves along with it. This type of mesh is generally used in computational solid mechanics.

In the Eulerian Mesh description, the mesh is fixed in space and the material moves through this fixed mesh, in other word, the motion of the material happens through the mesh instead of the mesh moving along with the material
The Arbitrary Lagrangian Eulerian (ALE) mesh is a combination of the Lagrangian and Eulerian type mesh where, the mesh is allowed to move in an arbitrarily specified way.

The nature of the material failure in machining is generally 'shear' but, it has been shown through careful studies and experimental observations that some amount of compressive stress is also involved during workpiece deformation. The thickening of the chip after cut is one such observation. The cutting forces which are incurred during machining can be classified into two categories. First, the shearing force and second, the ploughing force [5]. The description of ploughing force can be contrasted with the description, as presented, in the PiisPanen card model of the process where, only shearing is considered [6]. The tool nose radius plays a significant role in the magnitude of the cutting forces incurred during the machining operation [14-15].

It has been observed that with the decrease in the undeformed chip thickness the effect of ploughing becomes more significant. In the analysis carried out by P.K. Basuray et al. [7] it was noticed that, as long as the undeformed chip thickness remained smaller than the chip thickness, no

Corresponding Author: Ambrish Singh, Tel: +91 8989586724
Email: iambrishsingh@gmail.com

Contents lists available at http://www.jmsse.org/ & http://www.jmsse.in/

shearing force was incurred and the energy was expended in ploughing alone. Figure 1 given below shows these forces.

The ploughing force as suggested by P. Albrecht is the result of finite sharpness of the tool. As the tool nose radius is increased the ploughing force increases as well. This increment of force was also observed in the finite element simulation presented here.

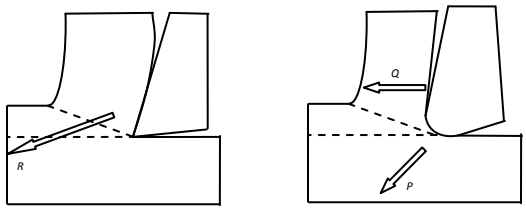

(a) (b)

Figure 1: Cutting Force Models (a) showing the force model involving shearing force only, (b) shows the force model involving both cutting force 'Q' as well as ploughing force 'P' [5]

Modeling considerations

CAD Modeling

The workpiece selected, was of rectangular box shape with dimensions 4mm × 3mm × 10mm. In order to achieve higher element density in the deformation zone as well as, for providing appropriate depth of cut during machining the workpiece was portioned into two cells. The material properties for the workpiece was that of Aluminium 6061-T6 alloy having a Young's Modulus of 650 GPa and a Poisson's ratio of 0.25. The tool however, was considered to be rigid and of shell nature. The deformation of the tool as compared with that of the workpiece is negligible thereby, validating the rigid body assumption. The rigid nature of the tool also facilitates lower computation time. Multiple simulations were performed using three different values of rake angle (i.e. -10^0, 15^0, 30^0), four different values of nose radius (i.e. 0, 0.1, 0.4, 0.6mm) and two different values of 'depth of cut' (i.e. 0.5 and 1mm). The variation in the parameter under study was made by holding other parameters constant for the simulation. The value of flank clearance angle was taken to be 5^0 for all the simulation.

Finite Element Modeling

The simulation of machining requires a governing model to address all the different aspects of the process; chip separation from the workpiece is one such aspect. The mesh that primarily defines the workpiece before deformation should be able to define the chip, along with the workpiece after deformation. The separation of chip from the workpiece can be addressed in many different ways [13, 16] some of them are discussed here.

Mesh With Iterative Re-Zoning

The Lagrangian mesh can be used with iterative rezoning [8], implying, the mesh used to discretize the workpiece and the chip for an interval of time 't' is replaced by a different mesh for the next interval of time 't + Δt'. The distribution of stresses and strains represented by the old mesh is interpolated onto the new mesh. This ensures that the new mesh is updated in terms of stress and strains fields. The new mesh however, does not retain any of the distortions the old mesh underwent due to the advancement of the tool towards the workpiece for that, particular time increment for which, it was used. This technique of continuous re-meshing between displacement increments of the tool avoids the problem of failed analysis due to excessive element distortion. The method of iterative rezoning or adaptive meshing even though effective, has some drawbacks. The process of re-meshing after every tool increment increases the computation time especially while simulating the process in three dimensions. Also, the transfer of data related to the stress and the strain distribution between the old and the new mesh takes place in an approximate form which introduces some amount of error in the simulation [1].

Geometric Chip Separation Criteria

A geometric chip separation criterion [9] achieves chip formation by implementing the condition of node separation after a certain predefined distance between the tool tip and the node is achieved. After the node separation the model undergoes a rezoning step. This rezoning step is required because of the fact that after node separation, the node, which was previously a part of the workpiece, becomes a part of the chip. This criterion is explained in the Fig. 2 where, d is the distance between the tool tip and the node and d_c represents the critical distance between the tool tip and the node after which, node separation occurs. Once this critical distance is achieve the node separates from the workpiece and becomes a part of the chip. This method of geometric chip separation followed by rezoning has been demonstrated to predict the cutting forces to an acceptable degree of accuracy. However, with this model the effect of the nose radius of the tool in the machining process is generally ignored.

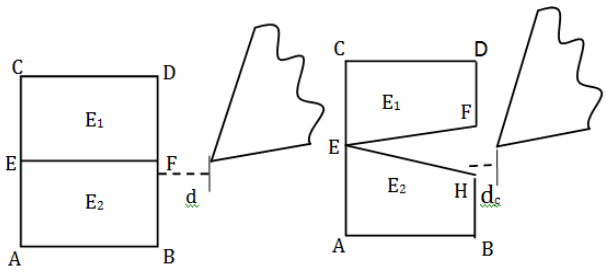

Figure 2: Diagram representing geometric chip separation criteria. (a) the distance between tool tip and the node is greater than critical distance ($d > d_c$), (b) the distance between the tool tip and the node is equal to the critical distance ($d \leq d_c$)

Lagrangian Mesh with Element Deletion

A Lagrangian mesh is generally used for models with low deformation. In order to successfully employ Lagrangian mesh where high deformations are involved without re-meshing, such as, machining the mesh has to be used along with a damage model [2, 10]. The damage model that was employed here, namely the Johnson Cook material damage model has been briefly discussed in the next section. The Johnson cook damage model defines a damage parameter 'D', where 'D' is described as follows.

$$D = \Sigma \frac{\Delta \varepsilon}{\varepsilon^f} \qquad (1)$$

Contents lists available at http://www.jmsse.org/ & http://www.jmsse.in/

'Δε', is the incremental strain corresponding to a particular time interval of the specific cycle of integration. 'ε^f ($\varepsilon_{Faliure}$)' is the strain to failure whose value is calculated using the equation 03 given in the next section. As the value of Δε becomes equal to the value of ε^f, damage parameter takes a value of unity. When the value of damage variable reaches 1 the stiffness of the material is considered to be fully degraded. As the stiffness of the element goes to zero, the element is simply deleted thereby, avoiding the simulation failure due to excessive element distortion. This deletion of the element also results in the formation of the chip, which flows over the rake face of the tool. A detailed description of the mesh that was used in the analysis is given in the following section.

Current Mesh Description

The mesh used to discretize the workpiece and the tool is a non uniform mesh. A non uniform mesh ensures improved results at moderate computation time by increasing the element density in the regions of high deformation while keeping the element density low in the regions of low deformation. The element density can be specified by the user either by specifying the number of elements (by changing edge or the part seed values in ABAQUS) that are to be used to discretize the region or by specifying the size of the elements for the discretization of the region.

The type of element that was used for the discretization of the workpiece was an 8-node linear brick element with approximate global size of 0.0005m. The element control in ABAQUS was set to structured hexagonal mesh. The element is named C3D8R in the ABAQUS software. The cutting tool as shown below has a nose radius; this nose radius of the cutting tool provides strength to the tool by reducing stress concentration at the tool tip during machining. In order to resolve the curvature on the cutting tool the number of elements at the tool tip had to be increased, as shown in Fig. 3.

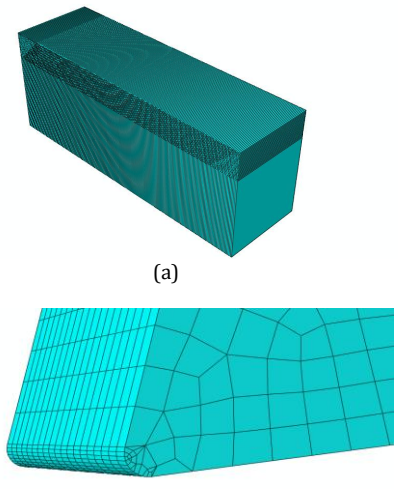

(a) (b)

Figure 3: Mesh Description. (a) shows the discretized geometric model of the workpiece and the tool. Along the length in the deformation zone (and the workpiece) the number of used elements are 200 along the height however, 20 elements are used, (b) The number of elements used for the discretization of the nose radius at the tool tip are 10, increasing the element density at the tool tip

Boundary Conditions

The boundary conditions applied for the model were;

1. Fixing the base of the workpiece (as shown in figure 04), similar to the process of shaping or slotting (ENCASTREU1=U2=U3=UR1=UR2=UR3=0).
2. Providing a cutting velocity to the tool along the length of the workpiece (V1 = -10)
3. Restriction of 'degrees of freedom' of the cutting tool i.e. displacement and rotation of the tool along the 'Y' and 'Z' direction (U2=U3=UR1=UR2=UR3=0).

Since the tool is a discrete rigid part the boundary conditions needs to be applied at the reference point. The tool was provided a cutting velocity of 10m/sec along the length of the workpiece (negative X direction) similar to the process of shaping. In order to enforce the cutting conditions the all degrees of freedom of the tool apart from the displacement in the X-direction were restricted. The restrictions of these degrees of freedom were essential to prevent the displacement and rotation of the tool under the influence of the forces developed during the cutting operation. The boundary conditions are represented in Fig. 4 given below.

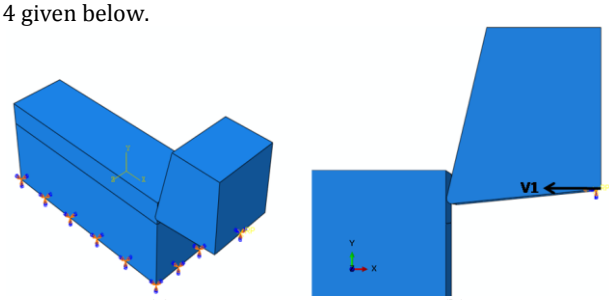

(a) (b)

Figure 4: Boundary Conditions, (a) showing the fixed base of the workpiece and (b) showing the direction of tool travel

Body Interaction

For the analysis presented here, kinematic contact method was used for enforcing the contact constraint. Also, contact pairs were specified in terms of 'master surface' of the tool and 'slave node region' of the workpiece. In case of rigid master surface the resisting force of all the slave nodes are applied as a generalized force in the associated rigid body. The tool rake surface and the nose radius were taken to be the "master surface" of the contact pair and the nodes of the deformation zone were taken to be the "slave" node region of the contact pair. For the interaction property the coefficient of friction was assigned a value of 0.3.

Johnson-Cook Material Model

Johnson-cook constitutive model [11] is generally used for materials subjected to large strains, high strain rates and high temperatures. The model is highly suited for simple and general computations as it uses variables which are readily available in most of the computer codes. For determining the constants of the strength equation which is given below (Equation 2) following test are needed to be performed. The results obtained from these tests can then be used to determine the constants, using techniques like curve fitting.

1. Torsion test over a wide range of strain rates.
2. Static tensile test

3. Hopkinson bar tensile test
4. Hopkinson bar tensile test at elevated temperatures

The model for the Von-Mises flow stress σ is expressed as

$$\sigma = [A + B\,\varepsilon^n]\ [1 + C\,ln(\dot{\varepsilon}^*)]\ [1 - (T^*)^m] \quad (2)$$

$$\text{Or, } \sigma = [A + B\,\varepsilon^n]\ [1 + C\,ln(\dot{\varepsilon}^*)]\ K_t \quad (3)$$

Where, $\dot{\varepsilon}^* = \dot{\varepsilon}/\dot{\varepsilon}_0$
$T^* = (T - T_{room}) / (T_{Melt} - T_{room})$
$K_t = [1 - (T^*)^m]$

The terms in the given equation are defined as follows: ε = Equivalent plastic strain, $\dot{\varepsilon}_0$ =Reference strain rate. Its value is generally taken as 1.0, $\dot{\varepsilon}$ =Strain rate, $\dot{\varepsilon}^*$= Dimensionless plastic strain rate for $\dot{\varepsilon}_0$=1.0 sec^{-1}, T^*=Homologous temperature, K_t =Thermal softening fraction, *A*, *B*, *C*, *n* and *m* = Material properties.

The expression in the first set of brackets gives the stress as a function of strain for the reference strain set to 1.0 and the homologous temperature set to 0. The expression in the second and third set of bracket represents the effect of strain rate and temperature respectively. The constants that depend on the material selected are mentioned as: *A* = Yield stress, *B*=Hardening Modulus (*B* and *n* represent the effect of strain hardening), *C*=Strain rate sensitivity coefficient/ Strain rate constant, *n*=Hardening coefficient, *m* = Thermal softening coefficient.

In the year 1985, Gordon R Johnson and William H Cook, in the journal of Engineering Fracture Mechanics published their paper on material damage model. The paper titled, "Fracture characteristics of three metals subjected to various strains, strain rates, temperature and pressures" presents this material damage model in detail. A short explanation of the model is given here. The damage to an element is defined as equation 1. Where, Δε = increment of equivalent plastic strain which occurs during an integration cycle. ε^f = Equivalent strain to failure.

When the value of D becomes unity fracture is said to have occurred.ε^f is obtained using the model proposed by Johnson and cook. The value of Δε upon reaching the value of ε^f in an incremental manner leads to the damage value of unity. The expression for the equivalent strain to failure (ε^f) is given below.

$$\varepsilon^f / \varepsilon_{Faliure} = [D_1 + D_2\ exp\ (D_3\sigma^*)]\ [1 + D_4\ ln\ (\dot{\varepsilon}^*)]\ [1 + D_5 T^*] \quad (4)$$

Where, $\sigma^* = \frac{\sigma m}{\sigma}$; σ_m is the average of the three normal stresses whereas, σ is the Von-Mises flow stress given in the equation 2.
$\dot{\varepsilon}^* = \dot{\varepsilon}/\dot{\varepsilon}_0$;$\dot{\varepsilon}$ is the strain rate and $\dot{\varepsilon}_0$ is the reference strain rate.
$\dot{\varepsilon}^*$ =Dimensionless strain rate, with the reference strain rate set to 1.0
T^* = Homologous Temperature.

D_1, D_2, D_3, D_4 and D_5 are the five material constants. The material failure model given above has three set of expressions. The expression in the first bracket represents the effect of hydrostatic stress on the strain to fracture. The expression in the second bracket represents the effect of strain rate on strain to fracture. The expression in the third bracket represents the effect of temperature on strain to fracture. The material damage constants are obtained by performing multiple experiments with wide range data for strain, strain rates and temperatures. The results from these experiments are then used along with the curve fitting technique to get the damage constants.

The table given below provides the Johnson Cook model parameters for the material strength and the material failure of Aluminium 6061-T6. The values for these constants were directly obtained from the literature [02].

1. Johnson-Cook material constants for Strength Model:

A (MPa)	B (MPa)	C	N	M
324.1	113.8	0.002	0.42	1.34

2. Johnson-Cook material constants for Fracture Model

D_1	D_2	D_3	D_4	D_5
-0.77	1.45	-0.47	0	1.6

Results and Discussion

Cutting force and Chip Morphology are the two most important indicators of overall machining quality. Also, cutting force is an important parameter for the 'condition monitoring' of both the cutting tool as well as the machine tool itself.

In order to successfully implement Finite element method in the cutting force investigation the variation in the magnitude of the cutting force with respect to the variations in the machining parameters should be studied. This not only helps in validating the model but it also points out the limitations of the model as well.

Following are the results obtained from the finite element simulation.

Cutting force variation with respect to tool rake angle

The simulation presented here was carried out for three different values of tool rake angle i.e. -10^0, $15^0$and 30^0. The corresponding value of cutting force is presented in Table 1.

Table 1: Cutting force value corresponding to tool rake angle

Rake Angle	Cutting force (N)
-10^0	1401
15^0	1115
30^0	877.7

As can be seen from the data given above, with the increase in tool rake angle the magnitude of cutting force decreases. Fig. 4 shows the cutting force variation throughout the machining simulation at different time steps.

Cutting force variation with respect to tool Nose radius

Nose radius is another important aspect of cutting tool geometry. Nose radius is generally provided to reduce the amount of stress concentration at the tool tip and to strengthen the tool. Cutting force analysis was carried out using four different values of nose radius and their corresponding maximum value of cutting force was recorded. The value of cutting forces corresponding to the values of nose radius is shown in Table 2.

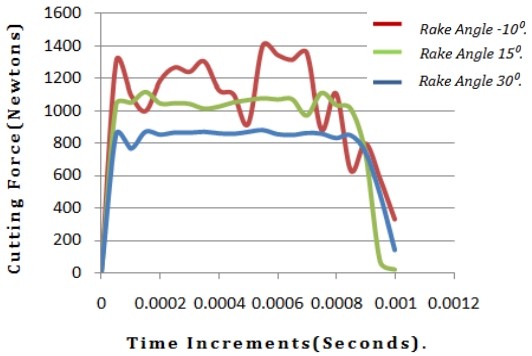

Figure 4: The cutting force variation with cutting tool rake angle set to -10^0, 15^0 and 30^0. The maximum value recorded for the cutting force were 1401, 1115, 877.7 Newton respectively

Table 2: Cutting force values corresponding to the value of tool nose radius

Nose Radius (mm)	Cutting Force (N)
0	1050
0.1	1115
0.4	1627
0.6	2085

The increment in the cutting force with increasing nose radius can be attributed to the fact that, as the tool nose radius increases the part of the cutting force generated because of the ploughing action becomes more significant leading to an increment in the overall value of the cutting force.

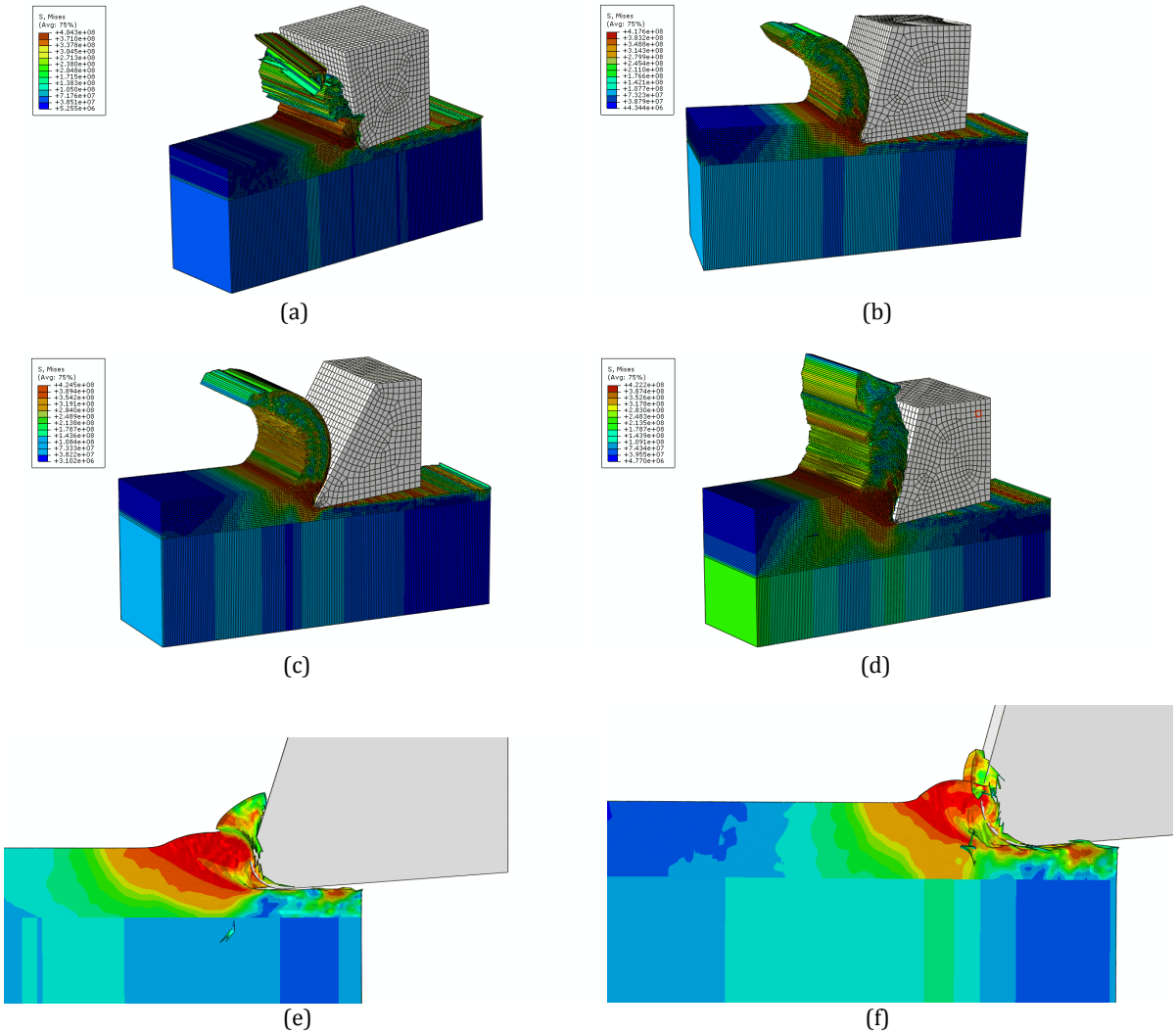

Figure 5: showing the tool with nose radius of 0.1mm and depth of cut of 0.5mm and the deformation of the workpiece at 0.00055seconds in the analysis with a rake angle of negative (a) 10^0, (b) 15^0, (c) 30^0, (d) 15^0, with depth of cut of 1.0 mm, (e) Tool Nose Radius = 0.4mm. The compressive nature of the cutting force during machining is demonstrated above, (f) Tool Nose Radius = 0.6mm. Increment in the tool nose radius increases the ploughing effect in the machining process

Cutting force analysis for 'depth of cut' variation

The magnitude of cutting force for depth of cut of 0.5mm and 1.0mm was 1115 N and 1688 N respectively. It is also important to note the values of reaction force at the fixed end of the workpiece. For 0.5 and 1.0mm depth of cut the reaction forces obtained were 58.8 N and 161.9 N respectively. This result signifies the importance of the rigidity of the machine tool while taking heavy roughing cuts.

In the following section the images obtained from the analysis is presented collectively. One can observe from the images, the chip morphology obtained from the machining simulation with different tool geometries (Figure 5). It must be noted that, the contour plots clearly show the distorted and segmented nature of chip while machining with a negative tool rake angle and the ploughing nature of the process while machining with a high tool nose radius. As the rake angle was increased the chip attained a more uniform and continuous shape. From Fig. 4, one can see the high fluctuations in the cutting force while machining with a negative rake angle tool, these fluctuations can be attributed to the non continuous and segmented nature of the chip. It must be pointed out that these observations are qualitative in nature and are in agreement with the experimental observations.

Conclusions

The results and observations made from the finite element analysis of the process of machining are in agreement with the experimental observations thereby, validating the model. The study successfully demonstrates that, using a Lagrangian Mesh with element deletion governed by, Johnson-Cook material failure and strength models can be successfully implemented for the study of machining process especially, for the investigation of cutting forces.

The trends in the cutting force variation with respect to the variations in tool rake angle and nose radius were accurately predicted by the model presented above.
A close observation of the contour plotsobtained by the analysis shows that, the material ahead of the cutting tool gets compressed before shearing or slip occurs. This phenomenon is more significant in tools with low or negative rake angles.

Increase in nose radius leadsto an increase in cutting force. This observation can attributed to the fact that with the increment in nose radius the value of ploughing force increases. A few qualitative observations made for the chip morphology that were in agreement with the experimental observations are as follows.

1. Increment in nose radius of the tool increases the compressive deformation of the material leading to a distorted and a segmented chip.
2. From graph on the cutting force generated by the negative rake tool one can see that, the smoothness of the curve as compared to the positive rake tools is low implying, large variations in the cutting force during machining. These variations induce vibrationsduring machining leading to poor quality of the job.

The analysis presented above even though reflects the trends in cutting force variation with respect to the variation in the machining parameters accurately, it must be noted that the experimental value of these forces may differ. This difference can be attributed to the assumptions and simplifications made in the analysis, for example ignoring the effect of temperature and changes in the material properties during machining. An attempt should be made develop a model encompassing all the aspects of machining.

References

1. Lars-Erik Lindgren, Ales Svoboda, Dan Wedberg, Mikael Lundblad, Towards predictive simulations of machining, C. R. Mecanique 2016, 344, 284–295.
2. I.S. Boldyrev, I.A. Shchurov, A.V. Nikonov, Numerical simulation of Aluminium 6061-T6 cutting and effect of constitutive material model and failure criteria on cutting forces' prediction, Procedia Engineering, 2016, 150, 866 – 870.
3. María H . Miguélez, Ana Muñoz - Sánchez, José L . Cantero, José A . Loya, An efficient implementation of boundary conditions in an ALE model for orthogonal cutting, Journal of theoretical and applied mechanics. applied mechanics, 2009, 47(3), 599-616.
4. Fabian Spreng, Peter Eberhard, Machining Process Simulations with Smoothed Particle Hydrodynamics", 15th CIRP Conference on Modelling of Machining Operations, Procedia CIRP, 2015, 31, 94 – 99.
5. P. Albrecht, New Developments in tie Theory of the Metal-Cutting Process, Journal of engineering for industry,1960.
6. Väinö Piispanen, Theory of Formation of Metal Chips, Journal of Applied Physics, 1948,19, 876.
7. P. K. Basuray, B. K. Misra and G. K.lal, Transition from plughing to cutting during machining with blunt tools, Wear, 1977, 43, 341 – 349.
8. V. Madhavan, S. Chandrasekar, T. N. Farris, Machining as a Wedge Indentation, Journal of Applied Mechanics, 2000, 67, 128-139.
9. A.G. Mamalisa, M. HorvaÂth, A.S. Branis, D.E. Manolakos, Finite element simulation of chip formation in orthogonal metal cutting, Journal of Materials Processing Technology, 2001, 110, 19-27.
10. Bing Wang & Zhanqiang Liu, Investigations on the chip formation mechanism and shear localization sensitivity of high-speed machining Ti6Al4V, Int J Adv Manuf Technol 2014 , 75, 1065–1076.
11. Gordan R. Johnson, William H. Cook, Constitutive model and data for metals subjected to large strains, high strain rates and high temperatures, In: Proc. 7th Int. Symp. On Ballistics, Hague, Netherlands, 1983, 541-547.
12. Gordan R. Johnson, William H. Cook, Fracture characteristics of three metals subjected to various strains, strain rates, temperatures and pressures, Engineering fracture mechanics, 1985, 21(1), 31-48.
13. J. Zouhar, M. Piska, Modelling the orthogonal machining process using cutting tools with different geometry, MM Science Journal, 2008, 48-51.
14. Y.B. Guo, Y.K. Chou, The determination of ploughing force and its influence on material properties in metal cutting, Journal of Materials Processing Technology, 2004, 148, 368–375.
15. Y. Kevin Chou, Hui Song, Tool nose radius effects on finish hard turning, Journal of Materials Processing Technology 2004, 148, 259–268.
16. H. Miguélez, R. Zaera, A. Rusinek, A. Moufki and A. Molinari, Numerical modeling of orthogonal cutting: Influence of cutting conditions and separation criterion, Journal de Physique IV, 2006, 134, 417-422.